Available online at www.sciencedirect.com
ScienceDirect
Physiological and Molecular Plant Pathology 68 (2006) 79–91
PMPP
www.elsevier.com/locate/pmpp

Differential gene expression in loblolly pine (*Pinus taeda* L.) challenged with the fusiform rust fungus, *Cronartium quercuum* f.sp. *fusiforme*

Henrietta Myburg[a], Alison M. Morse[b], Henry V. Amerson[a], Thomas L. Kubisiak[c], Dudley Huber[b], Jason A. Osborne[d], Saul A. Garcia[a], C. Dana Nelson[c], John M. Davis[b], Sarah F. Covert[e], Leonel M. van Zyl[a,*]

[a]*Forest Biotechnology Group, North Carolina State University, Raleigh, NC 27695, USA*
[b]*School of Forest Resources and Conservation, University of Florida, Gainesville, FL 32611, USA*
[c]*USDA-Forest Service, Southern Institute of Forest Genetics, 23332 Highway 67, Saucier, MS 39574, USA*
[d]*Department of Statistics, North Carolina State University, Raleigh, NC 27695, USA*
[e]*Daniel B. Warnell School of Forest Resources, University of Georgia, Athens, GA 30602, USA*

Accepted 3 July 2006

Abstract

Cronartium quercuum f.sp. *fusiforme* is the pathogen that incites fusiform rust disease of southern pine species. To date, a number of host resistance genes have been mapped. Although genomic mapping studies have provided valuable information on the genetic basis of disease interactions in this pine-rust pathosystem, the interaction at the molecular level is poorly understood. To further our understanding of this interaction, we implemented a microarray study to examine the differential expression of genes in pathogen-challenged progeny of a full-sib loblolly pine family known to be segregating at a single dominant resistance gene (*Fr1*). Statistical analyses revealed shifts in gene expression that may reflect discrete stages of gall development.

Keywords: *Cronartium quercuum* f.sp. *fusiforme*; Fusiform rust; Gene-for-gene interactions; Microarray analysis

1. Introduction

Southern pine species such as loblolly pine (*Pinus taeda* L.) and slash pine (*Pinus elliottii* Engelm. var. *elliottii*) have great economic value in commercial forestry operations in the United States and thus effective disease management is a priority. One of the most important tree diseases on these pine species is fusiform rust disease, incited by *Cronartium quercuum* (Berk.) Miyabe ex. Shirai f.sp. *fusiforme* (hereafter referred to as *Cqf*). This fungus affects normal wood development through a change in cellular differentiation and development [10,11]. These changes manifest at the macroscopic level as branch and stem galls. Stem galls lead to a reduction in wood quality and the generation of weak sections in the stem, making the trees vulnerable to wind damage. In cases where small trees and seedlings are severely galled, the disease can result in direct mortality, especially in slash pine.

Cqf is a biotrophic macrocyclic heteroecious fungus that infects both oaks and pines. Extensive research has been implemented to better understand the interaction between this pathogen and pine. In pines, selection and breeding for fusiform rust disease resistance and mapping of major resistance genes, such as the heterozygous *Fr1* gene reported by Wilcox et al. [28] in pine selection 10-5, has been undertaken to facilitate effective management of the disease and to reduce economic losses. Genomic mapping studies have identified a number of pathotype-specific resistance genes that confer resistance to fusiform rust disease [1,12,28, H.V. Amerson unpublished data]. However, these genomic mapping studies do not reveal the underlying molecular processes that occur in the host (either resistant or susceptible) when challenged with *Cqf* (Table 1).

*Corresponding author. Tel.: +1 919 961 6415; fax: +1 919 515 9813.
E-mail address: lmvanzyl@unity.ncsu.edu (L.M. van Zyl).

0885-5765/$ - see front matter © 2006 Elsevier Ltd. All rights reserved.
doi:10.1016/j.pmpp.2006.07.002

Table 1
Identification numbers, host origin, putative functions and *e*-values of clones listed in Figs. 3–5

Clone ID	Origin	Putative function/Top BLAST Hit	*E*-value[a]
G1	Fungal	Unknown function	
G2	Fungal	Unknown function	
G3	Fungal	**P32186** *Puccinia graminis* elongation factor 1-alpha	1e–71
G6	Fungal	Unknown function	
G8	Fungal	Unknown function	
G10	Fungal	**AAK96111** *Hebeloma cylindrosporum* glutamine synthetase	2e–67
G11	Fungal	Unknown function	
G12	Unknown	Unknown function	
G16	Fungal	**AAY30205** *Cronartium comandrae* ribosomal protein L12	5e–33
G18	Fungal	**P27800** *Sporidobolus salmonicolor* aldehyde reductase I	9e–19
G19	Fungal	Unknown function	
G30	Fungal	Unknown function	
G31	Fungal	Unknown function	
G32	Fungal	**DN910991** *Cronartium quercuum fusiforme* germinating basidiospore cDNA	0.0
G33	Fungal	**BAB43910** *Pholiota nameko* phosphate transporter	4e–14
G34	Fungal	**CV191748** *Puccinia graminis* infected wheat leaves	2e–43
G36	Unknown	Unknown function	
G37	Fungal	**EAA04378** *Anopheles gambiae* genomic sequence	4e–06
G39	Fungal	**AAW45184** *Cryptococcus neoformans* conserved hypothetical protein	4e–09
G41	Unknown	Unknown function	
G45	Unknown	**CN852221** *Pinus elliottii* infected with *Fusarium circinatum* cDNA (clone pi268)	7e–101
G50	Unknown	Unknown function	
G51	Pine	**DR071266** *Pinus taeda* dark roots EST	1e–155
G56	Unknown	Unknown function	
G57	Fungal	**ABA43719** *Xanthophyllomyces dendrorhous* beta-carotene oxygenase	1e–11
G59	Fungal	**XP_723102** *Candida albicans* vacuolar ATPase subunit C	3e–12
G65	Fungal	**DN911165** *Cronartium quercuum fusiforme* germinating basidiospore cDNA	2e–99
G66	Pine	**CN852416** *Pinus taeda* stem cDNA	2e–174
G67	Fungal	**AAP13580** *Lentinula edodes* guanine nucleotide binding protein beta subunit	1e–46
G68	Fungal	**XP_322575** *Neurospora crassa* 40S ribosomal protein S3	1e–18
G72	Fungal	**AAN76524** *Cryptococcus bacillisporus* heat-shock protein 90	1.5e–0
G75	Unknown	Unknown function	
H21	Pine	**CO362028** *Pinus taeda* needle EST	6e–152
DD62/J10	Fungal	Unknown function	
DD120/J4	Pine	**DR058329** *Pinus taeda* root EST	8e–168
pechi270 (= pi270)	Pine	**AAL58880** *Pinus elliottii* class IV chitinase	2e–44
pi107-2	Pine	**AJ784899** *Triticum aestivum* type 1 non-specific lipid transfer protein precursor[b]	8e–26
pi115-1	Pine	**AF410955** *Pinus sylvestris* antimicrobial peptide 4[b]	
pi117-1	Pine	**AF410955** *Pinus sylvestris* antimicrobial peptide 4[b]	
pi121-1	Pine	**DR102574.1** *Pinus taeda* resistant stem challenged with *Fusarium circinatum* cDNA	2e–66
pi129	Pine	**DR160114** *Pinus taeda* roots minus iron cDNA	1e–131
pi226	Unknown	Unknown function	
pi242	Pine	**BAA02724** *Glycine max* early nodulin	5e–17
pi243	Fungal	**NP_878121** *Saccharomyces cerevisiae* Ribonuclease H2 subunit Y1r154c-gp	1e–07
pi274	Unknown	Unknown function	
pi295	Pine	**AAT78791** *Oryza sativa* putative proteinase inhibitor	2e–09
pi315	Unknown	Unknown function	
pi54-5	Unknown	Unknown function	
pi57-2	Pine	**AF410955** *Pinus sylvestris* Antimicrobial peptide 4[b]	2e–107
pi64	Pine	**AAF60972** *Pseudotsuga menziesii* pathogenesis-related protein PsemI (PR10)	2e–26
Pic 56-12	Pine	**NP_177375** *Arabidopsis thaliana* ATL3 protein[b]	2e–23
NXCI 002 E07	Pine	**CAI56321** *Pinus taeda* leucoanthocyanidin reductase	4e–97
NXCI 008 C01	Pine	**BAA96365** *Bruguiera gymnorrhiza* oxygen evolving enhancer protein 1 precursor	5e–48
NXCI 018 A08	Pine	**CAA63496** *Musa acuminata* pectate lyase	1e–11
NXCI 033 F03	Pine	**AAX07432** *Pinus taeda* cytochrome P450 CYPB	6e–76
NXCI 042 D08	Pine	**DR385736** *Pinus taeda* roots plus mercury cDNA	7e–51
NXCI 069 A02	Pine	**AAF75826** *Pinus taeda* putative arabinogalactan/praline-rich protein	2e–14
NXCI 075 E11	Pine	**XP_465905** *Oryza sativa* putative mitochondrial NADH:ubiquinone oxidoreductase 29 kDa subunit	2e–14
NXCI 082 E07	Pine	**NP_912212** *Oryza sativa* putative xyloglucan endo-transglycosylase	6e–36
NXCI 084 G02	Pine	**AAC49545** *Pinus banksiana* alcohol dehydrogenase	8e–61
NXCI 094 E12	Pine	**AAF63756** *Vitis vinifera* pectate lyase	1e–33
NXCI 108 E05	Pine	**BG275820** *Pinus taeda* xylem side wood inclined cDNA	0
NXCI 150 F06	Pine	**AAM63331** *Arabidopsis thaliana* unknown protein	2e–16

Table 1 (*continued*)

Clone ID	Origin	Putative function/Top BLAST Hit	*E*-value[a]
NXCI 153 A02	Pine	Unknown function	
NXCI 153 F03	Pine	**DR683090** *Pinus taeda* embryo cDNA	0
NXCI 153 G06	Pine	**CAB72128** *Cucumis sativus* heat shock protein 70	9e–55
NXCI 155G05	Pine	**CF390005** *Pinus taeda* root cDNA	0
NXLV 039 H10	Pine	**AAC61287** *Arabidopsis thaliana* similar to gibberellin-regulated proteins	2e–20
NXLV 070 F01	Pine	**AAZ85375** *Solanum ochranthum* putative sterol C-14 reductase	1e–35
NXLV 077 B11	Pine	**AAC27845** *Arabidopsis thaliana* similar to gibberellin-regulated proteins	7e–08
NXLV 105 B02	Pine	**AAO61225** *Pinus taeda* (-)-alpha-pinene synthase	8e–117
NXLV 106 G06	Pine	**CAA70105** *Arabidopsis thaliana* Hsc70-G8 protein	9e–11
NXNV 007 G06	Pine	**AAS86762** *Lycopersicon esculentum* protein phosphatase 2C	5e–43
NXNV 028 A02	Pine	**AAP49840** *Arabidopsis thaliana* Gene info SAC domain protein 7	8e–51
NXNV 070 F06	Pine	**NP_913434** *Oryza sativa* putative PRLI-interacting factor N	2e–12
NXNV 083 E11	Pine	**AAO73433** *Citrus limon* vacuolar membrane ATPase subunit C	1e–24
NXNV 096 C08	Pine	**AAW21972** *Pinus monticola* Intracellular pathogenesis related protein PinmIII (PR10)	2e–32
NXNV 106 F12 F	Pine	**AW758897** *Pinus taeda* xylem cDNA	2e–137
NXNV 108 G08	Pine	**NP_918652** *Oryza sativa* genomic sequence P0520B06.18	7e–34
NXNV 128 D06 F	Pine	**AAC49718** *Pinus strobus* Pschi4 class I chitinase	1e–29
NXNV 135 E01	Pine	**NP_199066** *Arabidopsis thaliana* unknown protein	7e–19
NXNV 139 C11	Pine	**CAA65982** *Medicago sativa* cdc2MsF	1e–13
NXNV 151 A07	Pine	**CAE12163** *Quercus robur* expansin-like protein	2e–15
NXNV 162 H07	Pine	**AAD33596** *Hevea brasiliensis* thioredoxin h	1e–31
NXNV 173 C05	Pine	**ABA01483** *Gossypium hirsutum* gibberellin 3-hydroxylase 1	3e–55
NXPV 021 F10	Pine	**BAD95470** *Glycine max* BiP	1e–24
NXPV 025 E07	Pine	**AAB01550** *Picea glauca* late embryogenesis abundant protein	7e–15
NXPV 037 C02	Pine	**AAM28917** *Pinus taeda* putative TIR/NBS/LRR disease resistance protein	3e–10
NXPV 041 B08	Pine	**AAB68961** *Glycine max* protein kinase 3	7e–93
NXPV 068 E06 F	Pine	**AAN07898** *Malus x domestica* xyloglucan endotransglycosylase	3e–39
NXPV 076 C12	Pine	**DT634612** *Pinus taeda* embryo cDNA	3e–112
NXPV 078 G08	Pine	**BAD44306** *Arabidopsis thaliana* putative protein	6e–05
NXPV 133 B10	Pine	**DR118517** *Pinus taeda* Roots minus magnesium cDNA	1e–06
NXRV 003 H02	Pine	**CAH59451** *Plantago major* thioredoxin 2	4e–25
NXRV 060 D09 F	Pine	**CAD54618** *Pinus sylvestris* dehydrin	4e–09
NXRV 079 D01 F	Pine	**AAN07898** *Malus x domestica* xyloglucan endotransglycosylase	2e–60
NXSI 025 H02	Pine	**AAO61225** *Pinus taeda* (−)-alpha-pinene synthase	4e–41
NXSI 030 C06	Pine	**AAB66345** *Pinus taeda* calcium binding protein	3e–52
NXSI 044 C10	Pine	**U39405** *Pinus taeda* xylem 4-coumarate:CoA ligase	9e–64
NXSI 055 B06	Pine	**AAC32128** *Picea mariana* GASA5-like protein (gibberellin-regulated)	3e–40
NXSI 055 H08	Pine	**DR742053** *Pinus taeda* roots plus added copper cDNA	2e–174
NXSI 058 G02	Pine	**CAD54618** *Pinus sylvestris* dehydrin	1e–10
NXSI 098 A04	Pine	**XP_475872** *Oryza sativa* putative anti-silencing protein	3e–42
NXSI 098 C01	Pine	**AAR13288** *Gossypium hirsutum* annexin	8e–10
NXSI 099 H06	Pine	**AAO61228** *Pinus taeda* (+)-alpha-pinene synthase	3.66e–37
NXSI 103 E12	Pine	**AAF80590** *Asparagus officinalis* xyloglucan endotransglycosylase	3e–69
NXSI 113 E06 F	Pine	**AAN03485** *Prunus persica* xyloglucan-endotransglycosilase	8e–24
NXSI 118 F05	Pine	**AAX07432** *Pinus taeda* cytochrome P450 CYPB	7e–98
ST 25 C07	Pine	**NP_909983** *Oryza sativa* hypothetical protein	5e–20
ST 32 C09	Pine	**BAB02467** *Arabidopsis thaliana* protein with similarity to LEA protein	6e–32
23 G12	Pine	**Q96423** *Glycyrrhiza echinata* trans-cinnamate 4-monooxygenase	5e–55
40 D05	Pine	Dormancy associated protein	6e–21

[a]The *E*-value (expect value) is a parameter that describes the number of hits one can "expect" to see by chance when searching a database of a particular size.

[b]Putative functions were obtained through a blast query of a pine EST sequence instead of the original cDNA sequence. The original cDNA sequences were too short to give significant hits. Alignment between the original short cDNA and longer EST was manually checked before BLAST submission.

An assembly of molecular tools is now available to identify genes differentially expressed in the host after pathogen invasion. Warren and Covert [27] used differential display-reverse transcriptase PCR (DDRT-PCR) to identify pine genes that showed altered expression after *Cqf* infection as well as to identify *Cqf* genes that were expressed during gall formation. They identified six pine and 13 fungal cDNA clones with putative functions indicating involvement in plant development, plant defense and fungal stress responses.

Another study [23] focused on the application of differential display (DD) and suppression subtraction

hybridization (SSH) to identify pine genes potentially involved in host response to infection by *Fusarium circinatum* Nirenberg and O'Donnell. The genes that show significant regulation in response to challenge by *F. circinatum* were not derived from the SSH libraries constructed from *Cqf*-challenged tissues. This might be explained by the fact that biotrophic fungi, such as *Cqf*, require live host cells to complete their lifecycle and thus induce long-term suppression of the host's disease defense system [21] while necrotrophic fungi, such as *F. circinatum*, obtain nourishment from susceptible host cells killed during disease development and are tolerant to the delayed activation of defense genes in susceptible hosts. To identify the genes underlying these different types of plant–pathogen interactions as well as understand how they play a role in disease development, the differential expression of host genes from the initial time of infection through to full expression of disease symptoms needs to be studied.

Recently, microarray analysis has been used to study large-scale changes in gene expression over time. Gibly et al. [5] used SSH and microarray analysis to identify and study the expression of tomato genes that showed a differential regulation in a resistance response towards the tomato spot disease causal agent, *Xanthomonas campestris* pv. *vesicatoria*. The differentially expressed genes were classified into more than 20 main functional categories of which the largest included genes implicated in defense, stress responses, protein synthesis, signaling and photosynthesis.

The focus of our study was to examine the differential expression of genes in seedlings of a full-sib family of loblolly pine challenged with a single isolate of *Cqf* avirulent towards *Fr1* resistance. A crucial aspect of this study was our ability to genotype these using genetic markers predictive of segregation at the *Fr1* locus. The ability to predict the resistance genotype (*Fr1* allelic inheritance), and hence the expected phenotype of the seedlings prior to performing the inoculations, allowed us to study differential gene expression between the compatible and the incompatible interactions, even at time points preceding the manifestation of the disease phenotype. Tissues were harvested from sets of seedlings over a period of 4 months thus making it possible to follow the progression of the disease and the host–pathogen interaction at a molecular level from just minutes after pathogen challenge through to the point where the disease phenotype was completely visible.

2. Materials and methods

2.1. Plant material, genotyping and harvesting

Progeny from a loblolly pine full-sib family (10-5 ♀ × 4666-4 ♂) known to be segregating at a single dominant resistance gene (*Fr1*) were used as host plant material in the current study. Seeds from this family were cold stratified and then germinated in vermiculite trays, with seedlings initially maintained at North Carolina State University (NCSU) according to methods outlined in [16]. Megagametophyte DNA from each progeny was screened for RAPD markers J7_470 and AJ4_420 that are tightly linked to each other and to the heterozygous *Fr1* resistance gene in tree 10-5 at a distance of 1-2 cM (H.V. Amerson, unpublished data). RAPD reactions for the current study consisted of 15 μl reactions containing 15 μg non-acetylated bovine serum albumin (New England Biolabs, Inc. Beverly, MA), 1.5 mM $MgCl_2$ (Promega Corp. Madison WI), 1.5 μl 10X PCR buffer (100 mM Tris, 500 mM KCl, 1% Triton-X100, pH 9.0 adjusted with HCl), dNTPs (200 μM each dATP, dCTP, dGTP, dTTP), 30 ng 10 base oligonucleotide primer, 5 ng DNA template, 1 unit *Taq* DNA polymerase, and molecular grade water to volume. Reactions were assembled in 96-well U bottom polyvinyl chloride plates (Becton Dickinson Co. Franklin, NJ). Each reaction was overlaid with 50 μl of mineral oil and the plate was briefly centrifuged at 2500 rpm prior to amplification in MJ-Research PTC-100 thermocyclers. The thermocycling profile consisted of 41 cycles of denaturation at 92 °C for 1 min; annealing at 35 °C for 1 min; and extension at 72 °C for 2 min, followed by an indefinite hold at 4 °C. Prior to agarose gel electrophoresis, each amplified sample received 2 μl of loading buffer (0.025% bromophenol blue, 40% sucrose and 20 ng/μl ethidium bromide) followed by a brief centrifugation at 2500 rpm. Amplified samples with loading buffer were loaded into 1.5% agarose gels containing 140–190 ng/ml ethidium bromide. The gels were made using 1X TBE and were electrophoresed in 1X TBE for approximately 5 h at 150 V, using Owl Scientific Model A3 horizontal electrophoresis systems (Owl Scientific, Cambridge, MA). DNA bands in the gel were visualized with ultra violet and recorded on thermal paper using a Stratagene Eagle EYE™ video imaging system (Stratagene, La Jolla, CA) and a Sony Video Graphic Printer.

Given that no significant resistance was inherited from the highly susceptible pollen parent [17], markers J7_470 and AJ4_420 in megagametophyte DNA of progeny from the study cross, fully challenged with an avirulent fungal isolate, are very highly predictive of disease phenotype (H.V. Amerson unpublished data). Based on the RAPD marker analyses, individual progeny were identified as either resistant (*Fr1/fr1*; +J7_470, −AJ4_420) or susceptible (*fr1/fr1*; −J7_470, +AJ4_420) and grouped into resistant (R) versus susceptible (r) classes. For each class, 350 progeny were available for study. At approximately 2 weeks post-germination, the seedlings were transferred from NCSU to the USDA Resistance Screening Center in Asheville, NC.

The 350 individuals in each of the resistant (R) and susceptible (r) classes were sub-divided with 210 individuals (15 seedlings × 2 biological reps × 7 time points) being challenged with *Cqf* and 140 individuals (10 seedlings × 2 biological reps × 7 time points) included as controls (inoculated with distilled water). An additional 20 seedlings were water inoculated and included in the study as index

plants. These index plants were marked with two black ink spots, one immediately below the apical bud and the other approximately 1.5 cm below the first spot. This area represented the target area where gall formation was expected to occur and was used to guide the harvesting of tissues prior to the development of any visible disease symptoms. The first harvest time point was 90 min after inoculation followed by additional harvests at 6 h, 24 h, 7 days, 28 days, 56 days and 112 days post-inoculation. The harvested stem tissues were immediately frozen in liquid nitrogen and transferred to the Forest Biotechnology Laboratory (NCSU), where they were maintained at −80 °C until assayed.

2.2. Fungal material and inoculation

Fungal inoculum consisted of basidiospores derived from a single aeciospore isolate of *Cqf* (SC 20-21, obtained from E.G. Kuhlman, USDA-FS, retired). This isolate, homozygous avirulent (*Avr1*/*Avr1*) towards *Fr1*, was used to inoculate seedlings in the resistant and susceptible classes. Inoculations were performed at the USDA Resistance Screening Center (Asheville, NC) using a standard screening center protocol with an adjusted inoculum concentration [16] based on the concentrated basidiospore spray technique [20]. Seedlings at 8 weeks post seed sowing were sprayed with an aqueous spore solution at a concentration of 100,000 basidiospores/ml. Control and index plants were inoculated with distilled water. Following inoculation, plants were incubated in the dark for 24 h (at 20 °C and 97% RH) and then moved into the greenhouse (15–30 °C).

2.3. Microarray preparation

1248 ESTs (cDNA) were selected from the NSF loblolly pine cDNA libraries (http://pine.ccgb.umn.edu/). The ESTs in these libraries are organized into functional categories and we selected ESTs emphasizing disease and defense responses from the following main functional categories: cell rescue, cellular communication, transcription and metabolism. Also included were 1500 ESTs (UniGene Set) from the NSF loblolly pine cDNA libraries [15,25]. This EST set represents genes that encode for cell wall proteins, proteins for intermediate metabolism, stress-related proteins, DNA–RNA binding proteins, hormone responsive proteins, disease responsive proteins, transporters and proteins for lipid metabolism. An additional 322 ESTs, provided by J.M.D. and S.F.C. were included on the array. These ESTs were identified using DD and/or SSH and are of pine and fungal origin. Negative controls were included on the array in the form of water blanks.

Clones containing individual ESTs were picked and inoculated into 96-well blocks containing 1 ml Magnificent Broth (MB) and ampicillin (final concentration 100 μg/ml). Blocks were incubated overnight at 37 °C in a shaking incubator. Glycerol back-ups and 10 × dilutions of the glycerol stocks were made for each plate and stored at −80 °C. Amplification of the plasmid inserts was completed in a reaction volume of 100 μl. The following primer sets were used to amplify the inserts according to the plasmid vector used: M13 forward and M13 reverse, LD forward and LD reverse, T7 mod (5′-CGA CGG CCA GTG AAT TGT AAT AC-3′) and Sp6 mod (5′-GGT GAC ACT ATA GAA TAC TCA AGC T-3′). Each PCR reaction included the following: 81.5 μl molecular grade water (Sigma), 2 μl of 10 × diluted glycerol stock, 10 μl PCR Buffer (10 ×), 2 μl dNTPs (10 mM), 0.5 μl Taq Polymerase (5 U/μl), 2 μl of each primer per set. Primer concentrations were as follow: 10 μM M13 forward and 10 μM M13 reverse, 10 μM LD forward and 10 μM LD reverse, 10 pmol/μl T7 mod and 10 pmol/μl Sp6 mod. Three different amplification protocols were followed according to the primer set used. M13 primer set: (95 °C, 5 min) × 1 cycle, (94 °C, 30 s; 57 °C, 1 min; 72 °C, 4 min) × 34 cycles, (72 °C, 10 min) × 1 cycle, (4 °C, ∞). LD primer set: (95 °C, 5 min) × 1 cycle, (94 °C, 30 s; 68 °C, 3 min) × 34 cycles, (68 °C, 3 min) × 1 cycle, (4 °C, ∞). T7 mod/Sp6 mod primer set: (95 °C, 5 min) × 1 cycle, (94 °C, 30 s; 60 °C, 30 s; 72 °C, 30 s) × 39 cycles, (72 °C, 5 min) × 1 cycle, (4 °C, ∞). Successful amplification and insert quality were verified and documented on 1% agarose-ethidium bromide gels.

PCR products were purified using Multiscreen PCR 96-well filtration plates (Millipore) and re-dissolved in 40 μl PCR grade water. An equal volume of DMSO (40 μl) was added to each purified PCR product and mixed. The 96-well format PCR/DMSO products were transferred to 384-well plates and spotted twice on Corning CMT-ULTRAGAPS^{TM} coated slides (Corning, NY) using an Lucidea Spotter (Amersham Biosciences, NJ). Subsequent to printing, DNA fragments were UV cross-linked at 250 mJ, baked for 2 h at 80 °C and stored at room temperature.

2.4. Target synthesis

Specimen samples were grouped by treatment (inoculum used and time collected) and genotype (R or r). RNA was extracted from the target area using a CTAB method [3] combined with the Qiagen RNeasy Plant Minikit (Qiagen Inc.). RNA concentrations were spectrophometrically determined. A minimum of 60 and 83 μg of RNA was obtained for each of the inoculated (I) and control (C) grouped samples, respectively. These minimum amounts were isolated from all samples at each timepoint except the 28 days samples which yielded insufficient amounts of RNA. This timepoint was therefore excluded from further study.

First strand cDNA synthesis was completed according to the amino-allyl (aa) labeling protocol [8] used by TIGR (The Institute for Genomic Research). Ten micrograms of RNA per treatment and genotype were aliquoted into a 96-well format. Reference RNA samples (RC and rC) were set up by pooling equal amounts of RNA from each control

timepoint to a total of 10 μg (in a volume of 9 μl). Two microliters of random hexamer primers (Invitrogen) were added to each of the RNA samples. The RNA/hexamer primer mix was incubated at 70 °C for 10 min and snap-frozen on ethanol-ice for 30 s. The following was prepared for each first strand reaction and added to the RNA/random hexamer sample: 4 μl 5 × first strand buffer, 2 μl 0.1 M DTT, 1 μl 20 × aa-dUTP mix and 2 μl SuperScript II Reverse Transcriptase (200 U/μl). The 20 × aa-dUTP mix consisted of the following: 0.1 μl dATP (100 mM) (Invitrogen), 0.1 μl dCTP (100 mM) (Invitrogen), 0.1 μl dGTP (100 mM) (Invitrogen), 0.06 μl dTTP (100 mM) (Invitrogen) and 0.08 μl aa-dUTP (50 mM) (Ambion). First strand cDNA synthesis was done overnight at 42 °C. RNA hydrolysis was done by adding 10 μl 1 M NaOH and 10 μl 0.5 M EDTA to each reaction and incubating it at 65 °C for 15 min. The pH was neutralized by adding 10 μl 1 M HCl to each hydrolyzed sample. Unincorporated aa-dUTP and free amines were removed by combining the clean-up procedure of TIGR with the Qiagen QIAquick 96-well PCR purification kit (Qiagen Inc.). The purified aa-labeled cDNAs were dried in a speedvac.

Cy3 and Cy5 color reactions were performed as described in the TIGR protocol. The aa-labeled cDNAs were resuspended in 4.5 μl 0.1 M Na_2CO_3 (pH 9) and 4.5 μl of the appropriate Cy dye were added. Color reactions were incubated in the dark at room temperature for at least an hour. After incubation, 35 μl 0.1 M NaOAc was added to each color reaction. Uncoupled Cy dye was removed using the Qiagen QIAquick 96-well PCR purification kit (Qiagen Inc.) and reactions were dried in a speedvac. The purified Cy3 and Cy5 labeled targets were stored in the dark at −20 °C.

2.5. Microarray hybridization and scanning

The labeled targets were combined according to the experimental design and redissolved in 80 μl hybridization buffer according to L.M. van Zyl (unpublished) and Brinker et al. [2]. Combined targets were denatured for 3 min at 95 °C, centrifuged for a few seconds and added to slides prepared for hybridization. A cover slip was placed on top of the hybridization solution and the slides incubated overnight in Corning incubation chambers (Corning, NY). Ten microliters of water were added to the incubation chambers to prevent evaporation during the overnight incubation at 42 °C in the dark. All post-hybridization (stringency) washes were performed according to L.M. van Zyl (unpublished) and Brinker et al. [2]. Washed slides were dried by centrifugation for 5 min at 500 rpm and stored in the dark until scanned.

Slides were scanned at a resolution of 10 μm using a ScanArray 4000 Microarray Analysis System (GSI Lumonics, MA). Both channels (Cy3 and Cy5) were scanned with the laser power and photo-multiplier tube set to balance the channels. Quantification of spot intensities for both channels was determined with QuantArray (GSI Lumonics, MA).

2.6. Experimental design and statistical analysis

A fully balanced incomplete block design [14] was used as the experimental design for this study (Fig. 1). Gene significance was estimated using the mixed model approach [29] that is integrated in the SAS Microarray solutions (SAS MAS) software package (SAS Institute Inc. SAS Institute, Cary, NC). The $\log_2$ transformed data (y_{ijk}) were normalized using the normalization model: $y_{ijk} = \mu + A_i + D_j + (A \times D)_{ij} + \varepsilon_{ijk}$, where μ is the sample mean, A_I represents array effect, D_j the effect of the dye, $(A \times D)_{ij}$ the effect of the interaction between the array and dye and ε_{ijk} is the stochastic error. Residual values derived from this model were incorporated into the gene-specific model: $r_{ijk} = \mu + A_i + T_j + N_k + \varepsilon_{ijk}$, where T_j is the effect that correspond to the jth treatment combination. T_1–T_{24} represent the effects of the $2 \times 2 \times 6 = 24$ combinations of inoculum, pine genotype and time. Various effects of interest, such as the main effect of time or the interaction of time and genotype were investigated by evaluating appropriately chosen contrasts among these treatment effects. N_k is the spot effect due to the multiple spotted positions of the clones on the microarray. Both of the models use PROC MIXED in SAS (SAS Institute Inc. SAS/STAT Software version 9, SAS Institute, Cary, NC).

The experimental design, with 2 inocula, 2 pine genotypes, and 6 time points, generated a total of 1,209,325 pairwise contrasts, 109,756 of which were significant ($\alpha = 0.05$) without adjustment for multiple testing. These contrasts were between time by inoculum by genotype least square means. Volcano plots with p-value cutoffs set at $0.05/4224 = 1.1 \times 10^{-5}$ were used to visualize differentially expressed genes in the various contrasts. The

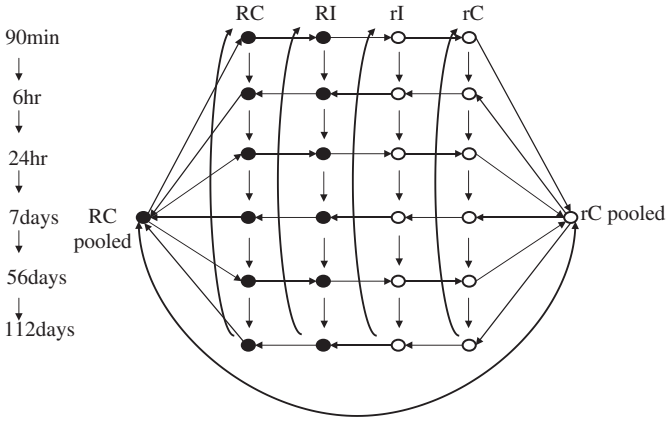

Fig. 1. Experimental design followed in this study. Treatment symbols are as follow: R = Resistant host, r = Susceptible host, C = Inoculation done with sterile water, I = Inoculation done with *Cqf* basidiospores isolate SC20-21, RC pooled = RNA from each RC sample at each time point pooled together, rC pooled = RNA from each rC sample at each time point pooled together. Each mRNA sample [represented by open (r) and closed (R) circles] was hybridized to 4 separate arrays labeled each with Cy3 and Cy5. Since arrays are represented by the arrows, the mRNA samples connected by an arrow are the samples hybridized to the array. Arrow orientation (head vs. tail) defines the labeling, i.e Cy 3→Cy 5.

highly significant gene list was generated using a *p*-value cutoff at the Bonferroni value of $0.01/1{,}209{,}325 = 1 \times 10^{-8}$ to assure an experiment-wise false discovery rate of 0.01. This yielded a list of 5087 significant contrasts. Figs. 3–5 were generated from datasets of highly significant genes that were parsed by inoculum, genotype and/or time (see Table 1 for gene list).

To validate the microarray results, we relied on the known ability of SSH to clone transcripts enriched in a tissue of interest. We predicted that the SSH clones derived from subtracting galled minus healthy transcript populations [27], would be greatly enriched in the rI 112 days treatment relative to rC, RI and RC treatments at 112 days. Indeed, clones obtained from the "galled" SSH library (designated "G" clones) [27] were prominent; a total of 32 "G" clones were declared highly significantly up-regulated in rI 112 days (out of a total of 62 "G" clones), whereas only one "H" clone showed this same pattern (out of a total of 47 "H" clones).

3. Results and discussion

3.1. Experimental implementation and significance

RAPD markers J7_470 and AJ4_420 allowed us to genotype the host material prior to the onset of the study and to assemble resistant ($R = Fr1/fr1$) and susceptible ($r = fr1/fr1$) host classes with respect to the *Fr1* locus. Each class consisted of 210 individuals that were challenged with basidiospores derived from the single aeciospore *Cqf* isolate (SC 20–21) known to be homozygous avirulent (*Avr1*/*Avr1*) towards *Fr1*. An additional 140 individuals from each class were sprayed with sterile water to serve as controls. An additional 20 "index plants" were sprayed with water and marked to guide the harvesting of the area where gall formation was most likely to occur.

Target stem regions were harvested over time, with the longest time being 112 days. At day 112, galls were clearly evident on all 30 of the seedlings classified as susceptible based on the RAPD markers. Conversely, none of the seedlings classified as resistant showed any visible disease symptoms. As expected, the susceptible trees' galls developed in the region predicted using the index plants. RAPD marker-based resistance genotyping was an essential prerequisite for this study. The ability to predict the resistance genotype (*Fr1* allelic inheritance), and hence the expected phenotype, of the progeny prior to performing the inoculations allowed us to study differential gene expression between the compatible interaction and controls at time points preceding the development of the disease phenotype, in contrast to previous studies that compared healthy and diseased seedlings after symptom development [23,27].

3.2. Gene expression during Cqf challenge

A main objective of this study was to identify genes significantly regulated over time in resistant (*R*) and susceptible (*r*) pines challenged with *Cqf*. Control groups (C), consisting of resistant and susceptible individuals, were mock inoculated to create a set of identical aged healthy trees for comparison. A total of 475 pine genes were identified as significantly regulated by treatment or time points. Approximately 30 fungal genes were detected during the later stages of disease development. To visualize differentially expressed genes in relevant contrasts as a whole, we used volcano plots in which fold regulation is plotted against statistical significance (Fig. 2A–D).

3.2.1. Highly significant genes

The distinct profiles of the volcano plots for the rI contrasts (susceptible-inoculated, right column of contrasts in Fig. 2) suggest that distinct genes are regulated over time, from early in the interaction prior to the appearance of disease symptoms, to much later in the interaction, when stem galls are manifest. Gene expression profiles during the pathogen infection stage (Fig. 2A) follow a similar trend between contrast (RC = RI = rC = rI), while during the stages of gall initiation (Fig. 2B) and gall expansion (Fig. 2C) the gene expression profile for the rI contrast was different versus the rest (RC = RI = rC $\neq$ rI). For example, a group of genes (indicated in blue) are present in the rI contrast during gall initiation and gall expansion stages and not seen in the other contrasts. The volcano plots for the 112d_90 min contrast (Fig. 2D) characterize the extremes of disease development, i.e., initial versus the final stages.

We now focus on genes whose expression was significantly different in one or more contrasts at $\alpha = 0.01$ after accounting for multiple testing using a Bonferroni step-down procedure. Focusing on these highly significant genes greatly enhances the likelihood of investigating true positives and dramatically reduces the list of regulated genes, thus facilitating biological interpretation.

We examined highly significant genes regulated during gall development over time (rI 112 days vs. rI 90 min; designated in Fig. 3 as gray bars) and in galled versus healthy stems of the same age (rI 112 days vs. rC 112 days; designated in Fig. 3 as black bars). There was a preponderance of genes that were up-regulated during gall development, as indicated by the small proportion of genes with negative $\log_2$-fold changes. As expected, many of the highly significant genes in common between these two contrasts (i.e., both gray and black bars) are pathogen-derived since both contrasts compare stems in diseased versus non-diseased states. The genes that are unique to the contrast between early and late time points (rI 112 days vs. rI 90 min; gray but not black bars) may either represent genes involved in stem development (since the contrast is between stems whose maturation state differs by 16 weeks) or previously unknown fungal genes. Genes unique to the contrast between galled and healthy stems of the same age (rI 112 days vs. rC 112 days; black but not gray bars) may represent either fungal genes or host genes whose expression is modulated by the biotrophic pathogen. To explore

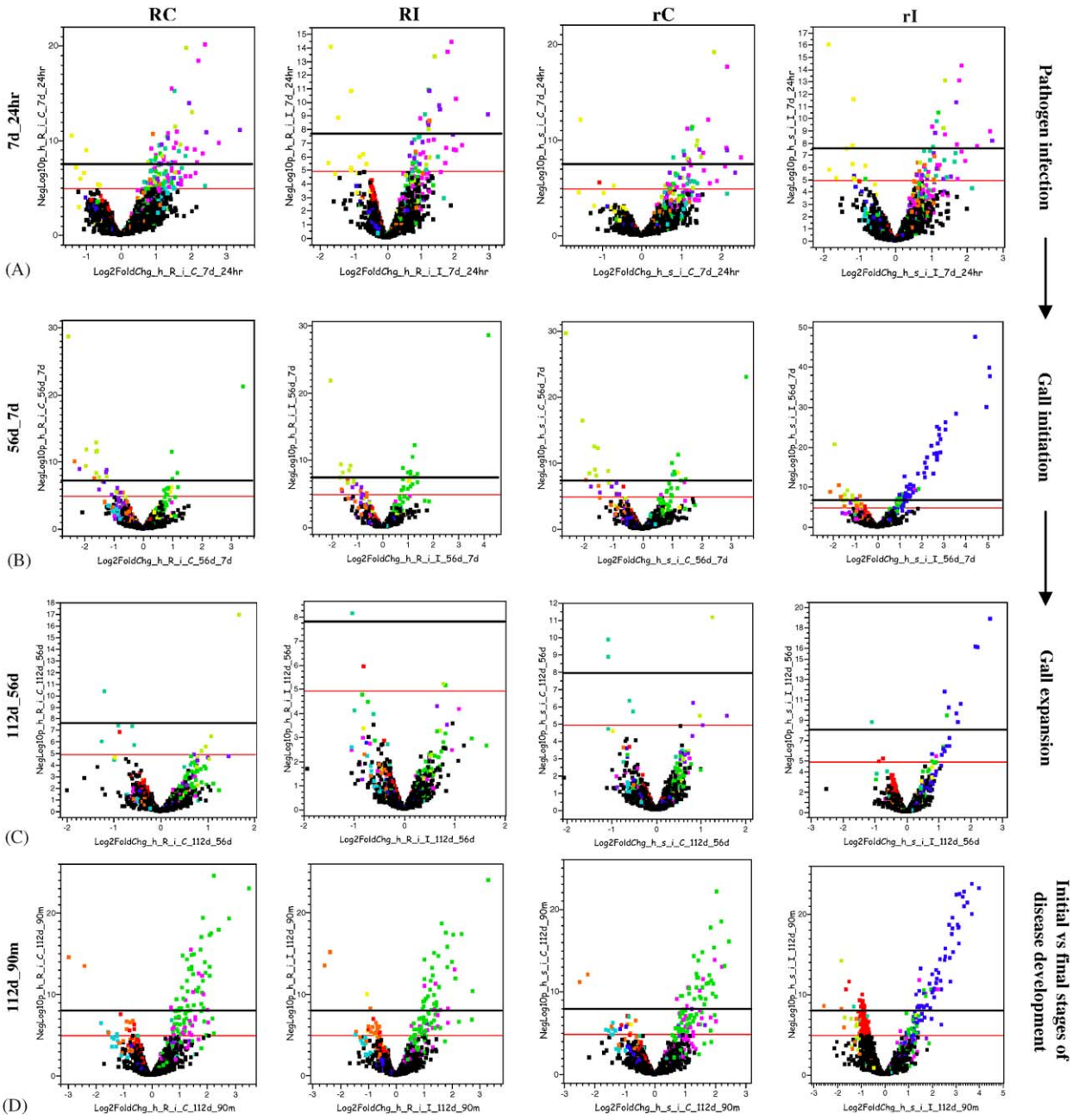

Fig. 2. Volcano plots present magnitude and direction of gene regulation (*x*-axis) vs. statistical significance of gene regulation (*y*-axis). Each volcano plot shows the $\log_2$ ratio of expression on the *X*-axis and the $-\log_{10}$ *p*-value of the ANOVA significance test on the *Y*-axis (cutoff = 1×10^{-5}, designated by the red horizontal line). Highly significant genes were selected using a more stringent *p*-value cutoff at the Bonferroni value of 1×10^{-8} to assure experimentwise false discovery rate of 0.01 (designated by the black horizontal line). Volcano plots for specific time comparisons are: (A) 7 days vs. 24h, (B) 56 days vs. 7 days, (C) 112 days vs. 56 days, (D) 112 days vs. 90min. Treatment symbols are as follow: R = Resistant host, r = Susceptible host, C = Inoculation done with sterile water, I = Inoculation done with *Cqf* basidiospores isolate SC20-21, RC pooled = RNA from each RC sample at each time point pooled together, rC pooled = RNA from each rC sample at each time point pooled together. Color coding reflects gene groups with similar expression levels and was identified by hierarchical clustering (data not shown) of significantly differentially expressed genes. In log scale captions h = host type, either R = resistant or s = susceptible and i = inoculum type, either I or C as above.

potentially interesting events within the full time course, we examined transitions in gene expression that occurred within shorter time frames.

3.2.2. *Stages of gall development*

The experimental design allowed us to distinguish between acute shifts in transcript abundance (significant regulation over short periods of time) and chronic shifts in transcript abundance (significant regulation over long periods). Fig. 4 reveals the patterns of regulation for 89 genes significantly regulated in the compatible interaction (contrasts between rI time points). These 89 genes (77 induced, 12 repressed) show either chronic or acute regulation, or both.

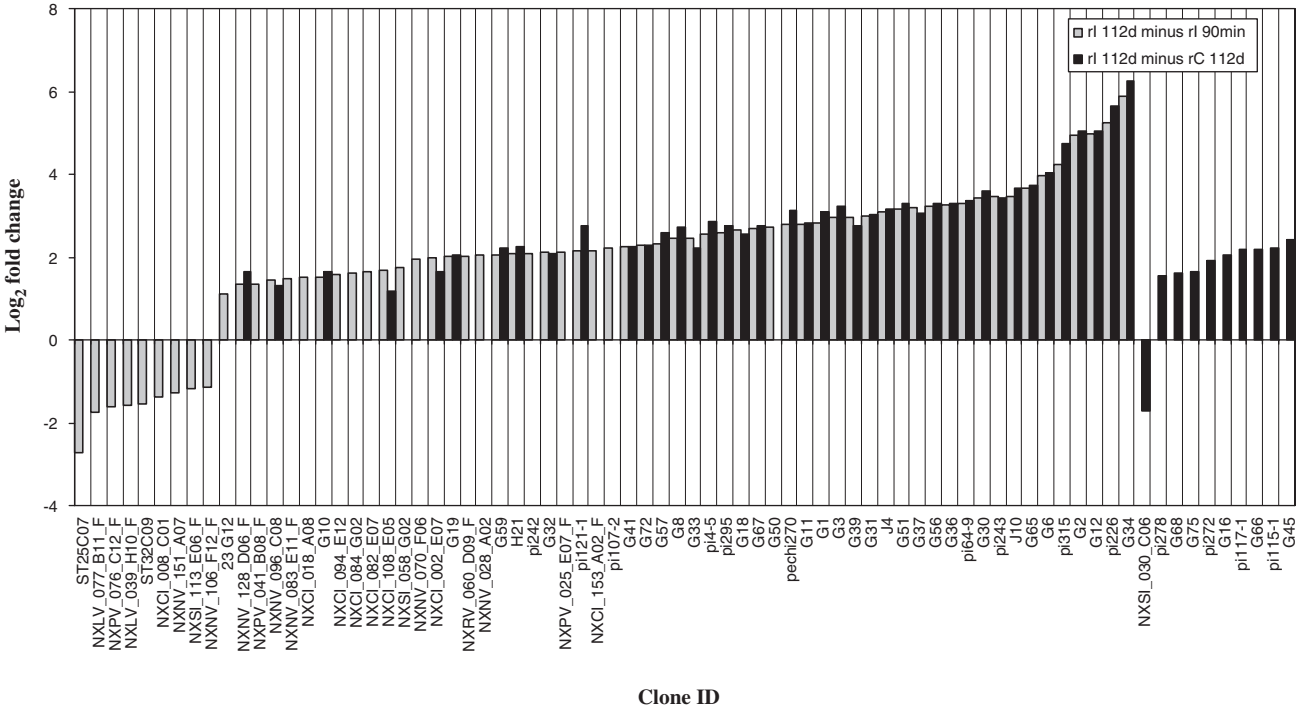

Fig. 3. Display of genes (*x*-axis) that are highly significantly regulated (alpha = 0.01, Bonferroni corrected) in contrasts between [rI 112d_rI 90min; gray bars] and [rI 112d_rC 112d; black bars]. These genes represent the contrasts of the full-blown disease state (rI 112d) compared to tissues that are either very young (rI 90min) or age-equivalent (rC 112d).

Twenty five of the induced genes (out of 77 total that were induced) were fungal in origin and are indicated as 'fungal' (Fig. 4). Interestingly, 16 of the 25 fungal genes were declared highly significant in the 7 days vs. 56 days contrast. We postulate that the acute increase in fungal transcript abundance during the interval from 7 to 56 days after challenge is indicative of high levels of fungal proliferation. The finding that none of the putative fungal genes were repressed supports this notion. We suggest this reflects ''gall initiation'' within 56 days of inoculation. This designation is consistent with histological observations regarding gall development in slash pine stems, where reaction parenchyma and distorted xylem, associated with gall formation were observed as early as 3 weeks after *Cqf* inoculation [22].

Of the remaining 64 regulated genes (89 total minus the 25 fungal genes), 12 were significantly repressed during the compatible interaction with eight acutely repressed at particular intervals (solid blue boxes in Fig. 4). Two genes showed both induction and repression at consecutive intervals. The remaining 52 genes revealed either chronic induction (hatched orange boxes connected by a line only), acute induction (solid orange boxes only), or both (hatched orange boxes connected by a line and solid orange boxes). It is notable that 19 genes were only induced in an acute fashion, meaning they were declared significant in an adjacent time interval but not declared significant in the contrast between 90 min and 112 days. Interestingly, most of these genes (14 out of 19) were regulated between 24 h and 7days, the interval just prior to acute accumulation of fungal transcripts. We suggest that since acute host transcript regulation preceded the acute accumulation of fungal transcripts, host tissues were responding to cues from the pathogen as a consequence of ''fungal infection'' within 1 week of inoculation. This is consistent with several previous studies of histological and ultrastructural observations that verified *Cqf* infection within one week of inoculation. In *Cqf* challenged pine hypocotyls, epidermal cells were infected at 24 h post-inoculation in loblolly pine [7] and infection was near the cambium at 1 week post-inoculation in slash pine [22]. Additionally, Gray and Amerson [6] showed that incompatible epidermal necrosis in loblolly pine hypocotyls challenged with *Cqf* could be detected at 36 h post-inoculation. Also, in a comparison of three *Cqf* inoculated seed lines deemed resistant, intermediate or susceptible (with regards to fusiform rust field resistance), incompatible necroses (epidermal, cellular and tissue) at 7 days post-inoculation were greatest in the resistant line [6].

A modest number of genes (NXNV_096_C08, pi295, pic54-5, and pi64) were acutely regulated during the last time interval tested, between 56 days and 112 days. The small number of acutely regulated genes during this interval may imply minimal global transcriptome shifts occur after the basic architectural plan for a gall has already been established. Alternatively, the array may not contain a large number of host genes involved in this stage of disease development. Based on observations of fusiform

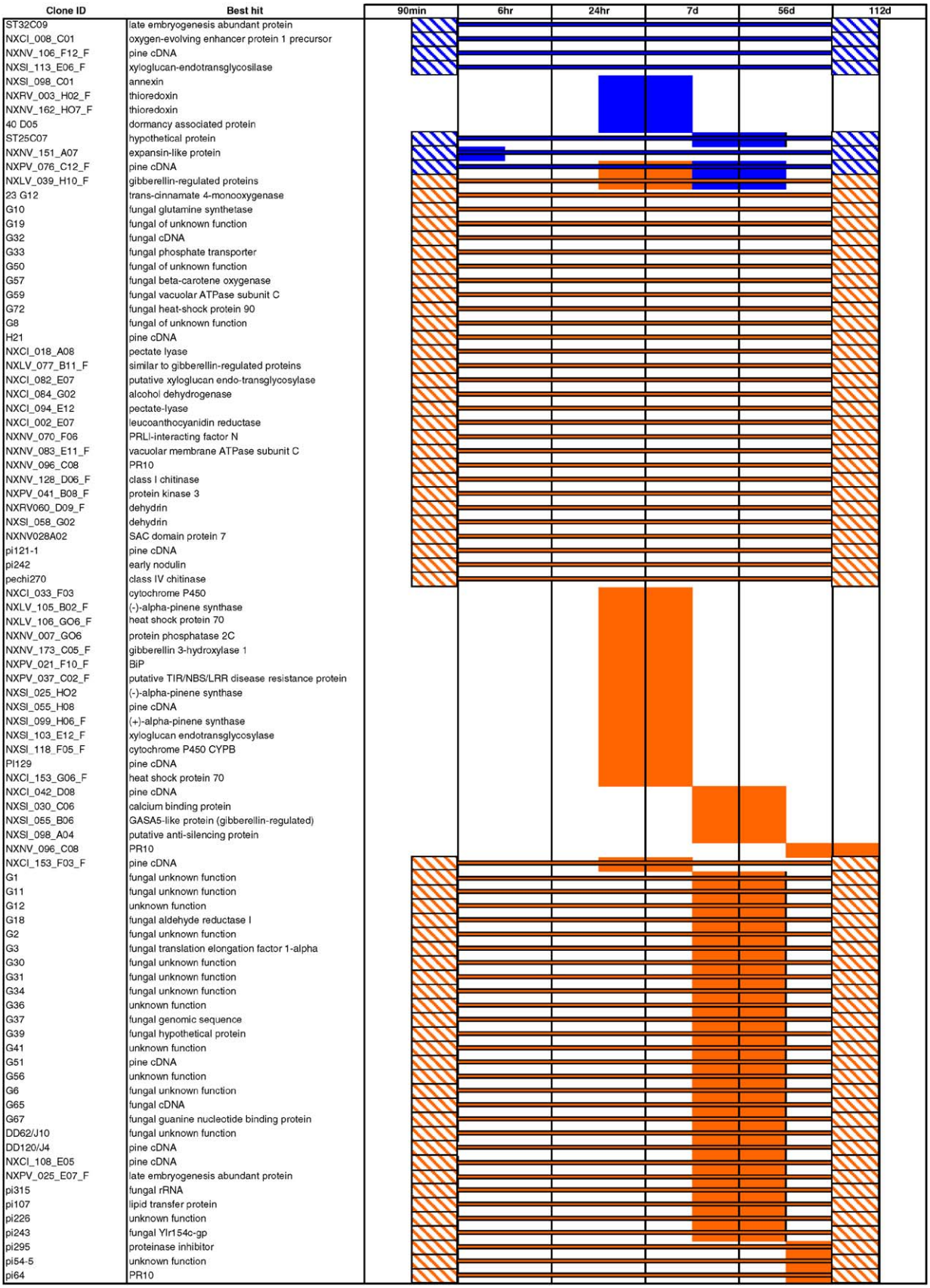

Fig. 4. Acute versus chronic shifts in gene regulation over time in the compatible interaction. Genes significant at sequential time points are indicated by thick solid bars under the appropriate time point(s). These are acute, stage-specific shifts in gene expression. Genes significant in the [rI 112d_rI 90min] contrast are indicated by hatched bars under the appropriate time points and joined by a thin solid bar. These are longer-term, slower shifts in gene expression that are only detected in "distant" contrasts. Blue = repressed, orange = induced.

rust gall development in this and other studies of loblolly pine, we suggest the interval between 56 and 112 days reflected "gall expansion."

3.2.3. Regulation and consequences of gall development

We hypothesize that the modulation of host genes during disease progression implies the presence of signals used by the pathogen to alter host stem development leading to gall formation. We speculate that *Cqf* either synthesizes gibberellins or exploits gibberellins in the host to modify host stem development to form a gall. This is based on our observations that four different highly significant genes are similar to gibberellin-regulated genes from *Arabidopsis thaliana* (NXLV_039_H10, NXLV_077_B11), *Picea mariana* (NXSI_055_B06) and *Gossypium hirsutum* (NXNV_173_C05). Interestingly, these genes are not co-regulated; NXLV_39_H10 was acutely induced in the contrast between 24 h and 7 days and repressed in the contrast between 7 and 56 days, NXNV_173_C05 was acutely induced only between 24 h and 7 days, NXSI_055_B06 was acutely induced only in the contrast between 7 days and 56 days, and NXLV_077_B11 was chronically induced. This may suggest action of gibberellins at multiple stages of gall development. Gibberellins have been identified in many species of plants, including the stems and needles of *Pinus sylvestris* [26] and pollen of *Pinus attenuata* [13] and exogenous application of gibberellins promoted epicotyl elongation and increased stem unit length in *P. sylvestris* and *Picea glauca* [18]. Transgenic trees engineered to have higher concentrations of gibberellins have increased radial and longitudinal growth, increased numbers of xylem fibers [4] and changes in the expression of genes associated with early xylogenesis [9]. Together, these results indicate that gibberellins play a role in the development of the woody stem and at multiple stages. Gibberellins are also present in plant pathogenic fungi where they were originally identified and received their name [30]. Our results establish a framework for testing the role(s) of gibberellins in fusiform rust gall development.

Four genes are similar to genes encoding late embryogenesis abundant (LEA) proteins, two of which belong to the dehydrin class of LEA proteins. The expression of LEA proteins in vegetative tissues is associated with osmotic stress. Both putative dehydrins identified in our study showed a chronic induction pattern. The LEA gene NXPV_025_E07 revealed an acute induction during the interval between 7 and 56 days as well as chronic induction. In contrast, ST_32_C09, the fourth LEA gene, showed a chronic repression pattern. We conclude that regulation of these LEA genes reflects altered vascular development incited by the pathogen resulting in shifts in water availability within the stem. Supporting this conclusion are magnetic resonance microscopy studies that show disruption of xylem water transport at the transition between the healthy tissue below a gall and galled tissues [19]. Other regulated genes encoding proteins with potential roles in stress or defense responses include PR10 proteins (pi64 and NXNV_096_C08), heat shock protein 70 s (NXCI_153_G06, NXLV_106_G06), class I and class IV chitinases (NXNV_128_D06, pi270), thioredoxins (NXRV_003_H02_F, NXNV_162_H07 F) and terpene synthases (NXSI_025_H02, NXLV_105_B02 F, NXSI_099_H06). The regulation of terpene synthases is intriguing since *Cqf* haustoria localize to parenchyma cells of the xylem and phloem and to epithelial cells surrounding resin ducts [10].

3.2.4. Modulation of host genes by the pathogen

We asked if the microarray experiment revealed influences of *Cqf* on host stem development. To test this, we identified 37 genes significantly regulated in one or more rC vs. rC contrast (Fig. 5). All of these genes must be host in origin since they were expressed in water-inoculated control plants. All show significant regulation at one or more stages of stem development, presumably reflecting processes of stem maturation in the transition between a young seedling with a succulent stem containing primary tissues (90 min) and older seedlings with a woody stem containing secondary tissues (112 days). We next examined regulation of these genes in the comparable rI vs. rI contrasts, to determine if regulation was altered in some fashion by *Cqf* (Fig. 5). There were numerous cases in which regulation was different between rC vs. rC and rI vs. rI contrasts for a given time point, however only eight were declared highly significant (t values >5; indicated by asterisks in Fig. 5). These eight instances of *Cqf*-influenced host gene regulation involved six genes. We consider it biologically relevant because all six genes were regulated significantly during stem development under control conditions, but were not regulated after pathogen inoculation leading to gall development. This implies *Cqf* maintenance of stem development in a more juvenile state, since the developmental trajectory of the stem—as reflected by shifts in gene expression in controls—was impeded. The specific biological roles played by the regulated genes is unclear because only one, encoding 4-coumarate:CoA ligase (NXSI_044_C10), has a direct connection to stem development through involvement in cell wall biosynthesis. Of the remaining 5 genes, three have unknown functions (NXPV_133_B10, pi274, ST_25_C07) and two, a putative PRL1-interacting protein (NXNV_070_F05) and a putative BiP (NXPV_021_F10), have not been linked to stem development *per se*. It is intriguing that PRL1 appears to function as an integrator of hormonal and sugar signaling pathways which may be modulated in developing stems [24].

The differential regulation of host genes during gall formation is not unexpected given the nature of the interaction between host and pathogen leading to fusiform galls. Fusiform rust galls undergo xylem hypertrophy, cellular dysplasia and modifications of annual growth rings that result from changes in host cell number as well as cell size and shape [10,11]. Interestingly, we did not identify

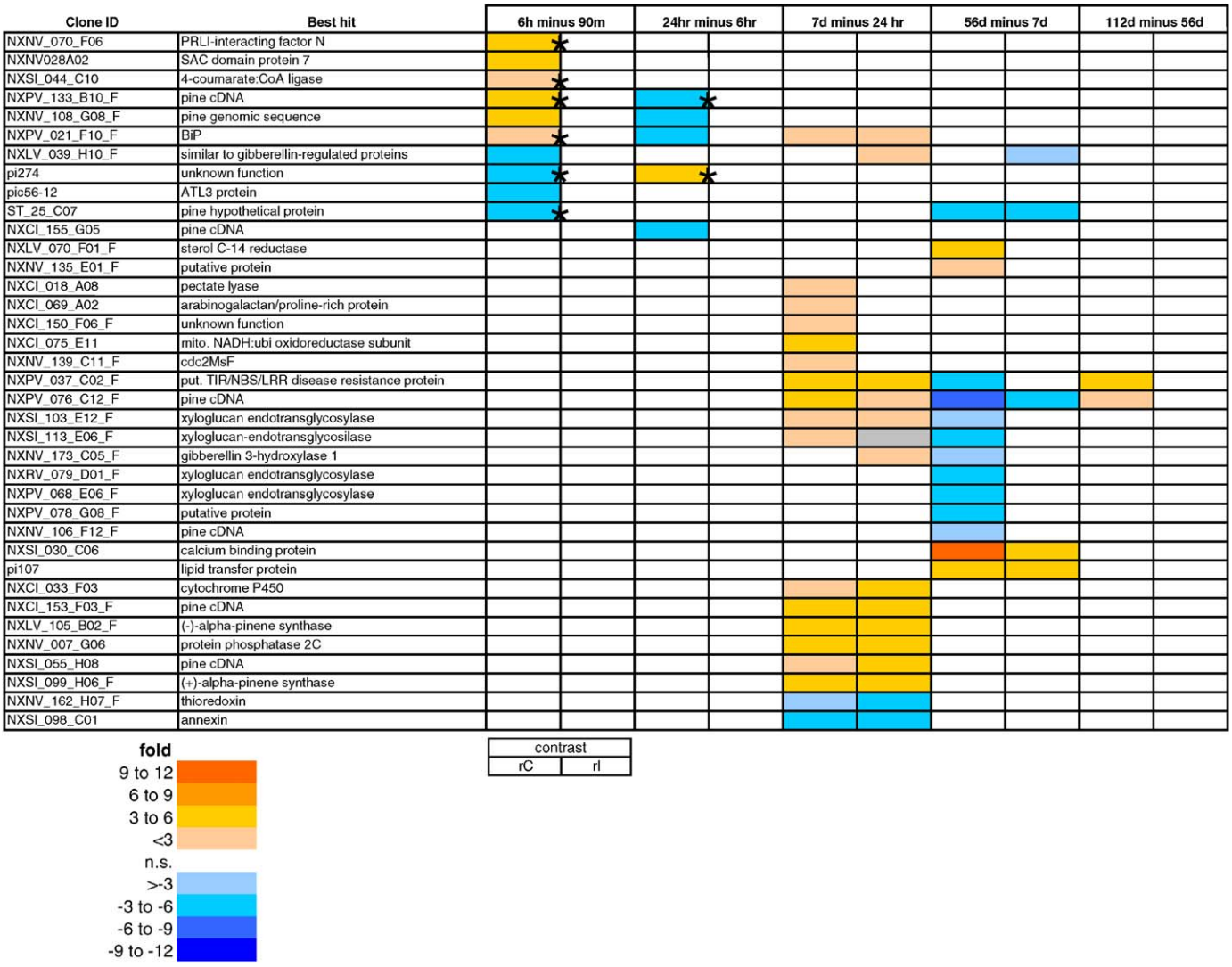

Fig. 5. Host gene regulation can be modulated by *Cqf*. Host genes significantly regulated during normal development were identified by virtue of their regulation within the rC treatment combination. Genes (rows) are shown according to the time contrasts (columns) in which they are significantly regulated. Each time contrast shows significance in rC_rC (left box) and significance in rI_rI (right box). Fold regulation is indicated by color intensities, with white indicating no significant regulation. An asterisk indicates a highly significant difference (t value >5) in the linear contrast [(rI_rI)_(rC_rC)], which verifies the influence of *Cqf* on host gene regulation.

significantly regulated genes in the incompatible interaction (RI vs. RC or rC). This could have been due to a number of factors. The most obvious, but highly unlikely, reason is that there were no genes differentially expressed during these early time intervals. Instead, we reason that this lack of differential gene expression might have been due to one or a combination of the following: (i) inappropriate timing of tissue harvest, (ii) low abundance of the appropriate gene transcripts and/or (iii) the possibility that the genes selected for array construction did not include those genes expressed during the incompatible interaction. These technical hurdles should be kept in mind and specifically addressed in future research efforts. The results presented here suggest that genes involved in stem development, being most prominent on the microarray platform used in this study, are altered in their regulation by pathogen derived signals. Significantly modulated genes are now targets for further investigation of these signals and their consequences.

Acknowledgments

This work was supported by the USDA Forest Service, Southern Research Station, Cooperative Agreement SRS 04-CA-11330126-020, USDA-CSREES-IFAFS Agreement 2001-52100-11315 (to LZM) and NSF-DBI Award 0501763 (to J.D.). H.M. was also financially supported by the National Research Foundation (South Africa). We thank Carol Young (USDA Forest Service, Resistance Screening Center, Asheville, NC) for outstanding technical service and assistance.

References

[1] Amerson H, Jordan AP, Kuhlman EG, O'Malley DM, Sederoff RR. Genetic basis of fusiform rust disease resistance in loblolly pine. In: Proceedings of the 24th southern forest tree improvement conference. 1997. p. 403.

[2] Brinker M, Van Zyl L, Liu W, Craig D, Sederoff R, et al. Microarray Analysis of gene expression during adventitious root development in *Pinus contorta*. Plant Physiol 2004;135:1526–39.

[3] Chang S, Pryear J, Cairney J. A simple and efficient method for jjisolating RNA from pine trees. Plant Mol Biol Rep 1993;11:113–7.

[4] Eriksson ME, Israelsson M, Olsson O, Moritz T. Increased gibberellin biosynthesis in transgenic trees promotes growth, biomass production and xylem fiber length. Nature Biotech 2000;18:784–8.

[5] Gibly A, Bonshtien A, Balaji V, Debbie P, et al. Identification and expression of tomato genes differentially regulated during a resistance response to *Xanthomonas campestris* pv. *vesicatoria*. Mol Plant–Microbe Interact 2004;17:1212–22.

[6] Gray DJ, Amerson HV. In vitro resistance of embryos of *Pinus taeda* to *Cronartium quercuum* f. sp. *fusiforme*: ultrastructure and histology. Phytopathology 1983;73:1492–9.

[7] Gray DJ, Amerson HV, Van Dyke CG. Ultrastructure of the infection and early colonization of *Pinus taeda* by *Cronartium quercuum* f. sp. *fusiforme*. Mycologia 1983;75:117–30.

[8] Hegde P, Qi R, Abernathy K, Gay C, Dharap S, Gaspard R, et al. A concise guide to cDNA microarray analysis. Biotechniques 2000;29: 548–56.

[9] Israelsson M, Eriksson ME, Hertzberg M, Aspeborg H, Nilsson P, Moritz T. Changes in gene expression in the wood-forming tissue of transgenic hybrid aspen with increased secondary growth. Plant Mol Biol 2003;52:893–903.

[10] Jackson LWR, Parker JN. Anatomy of fusiform rust galls on loblolly pine. Phytopathology 1958;48:637–40.

[11] Jewell FF, True RP, Mallett SL. Histology of *Cronartium fusiforme* in slash pine seedlings. Phytopathology 1962;52:850–8.

[12] Jordan AP. Fusiform Rust Disease Resistance and Genomic Mapping in Loblolly Pine. 1997. Master's thesis, North Carolina State University, Raleigh, NC.

[13] Kamienska A, Durley RC, Pharis RP. Isolation of gibberellins A_3, A_4 and A_7 from *Pinus attenuata* pollen. Phytochemistry 1976;15:421–4.

[14] Kerr MK, Churchill GA. Experimental design for gene expression microarrays. Biostatistics 2001;2:183–201.

[15] Kirst M, Johnson AF, Bausom C, Ulrich E, Hubbard K, Staggs R, et al. Apparent homology of expressed genes from wood-forming tissues of loblolly pine (*Pinus taeda L.*) with *Arabidopsis thaliana*. Proc Natl Acad Sci USA 2003;100:7383–8.

[16] Knighten JL, Young CH, McCartney TC, Anderson RL. Resistance screening center procedures manual: a step-by-step guide used in the operational screening of southern pines for resistance to fusiform rust. USDA Forest Service Pest Management report 83-1-18, 1988.

[17] Kuhlman EG. Interaction of virulent single-gall rust isolates of *Cronartium quercuum* f.sp. *fusiforme* and resistant families of loblolly pine. For Sci 1992;38(3):641–51.

[18] Little CHA JE, MacDonald. Effects of exogenous gibberellin and auxin on shoot elongation and vegetative bud development in seedlings of *Pinus sylvestris* and *Picea glauca*. Tree Physiol 2003; 23:73–83.

[19] MacFall JS, Spaine P, Doudrick R, Johnson GA. Alterations in growth and water-transport processes in fusiform rust galls of pine, determined by magnetic resonance microscopy. Phytopathology 1994;84:288–93.

[20] Matthews FR, Rowan SJ. An improved method for large-scale inoculation of pine and oak with *Cronartium quercuum*. Plant Dis Rep 1972;56:931–4.

[21] Mendgen K, Hahn M. Plant infection and the establishment of fungal biotrophy. Trends Plant Sci 2002;7:352–6.

[22] Miller T, Cowling EB. Infection and colonization of different organs of slash pine seedlings by *Cronartium fusiforme*. Phytopathology 1977;67:179–86.

[23] Morse AM, Nelson CD, Covert SF, Holliday AG, Smith KE, Davis JM. Pine genes regulated by the necrotrophic pathogen *Fusarium circinatum*. Theor Appl Genet 2004;109:922–32.

[24] Németh K, Salchert K, Putnoky P, Bhalerao R, Koncz-Kálmán Z, Stankovic-Stangeland B, et al. Pleiotropic control of glucose and hormone responses by PRL1, a nuclear WD protein, in *Arabidopsis*. Genes Dev 1998;12:3059–73.

[25] Stasolla C, Van Zyl LM, Egertsdotter U, Craig D, Lui W, Sederoff R. The effects of polyethylene glycol (PEG) on gene expression of developing white spruce somatic embryos. Plant Physiol 2003;131: 1–12.

[26] Wang Q, Little CHA, Moritz T, Oden PC. Identification of endogenous gibberellins, and metabolism of tritiated and deuterated GA_4, GA_9, and GA_{20} in Scots pine (*Pinus sylvestris*) shoots. Physiol Plant 1996;97:764–71.

[27] Warren JM, Covert SF. Differential expression of pine and *Cronartium quercuum* f. sp. *fusiforme* genes in Fusiform Rust Galls. App Environ Microbiol 2004;70:441–51.

[28] Wilcox PL, Amerson HV, Kuhlman EG, Liu B- H, O'Malley DM, Sederoff RR. Detection of a major gene for resistance to fusiform rust disease in loblolly pine by genomic mapping. Proc Natl Acad Sci USA 1996;93:3859–64.

[29] Wolfinger RD, Gibson E, Wolfinger L, Bennett H, Hamadeh P, Bushel C, et al. Assessing gene significance from cDNA microarray expression data via mixedmodels. J Comput Biol 2001;8:625–37.

[30] Yabuta T. Biochemistry of the "bakanae" fungus of rice. Agric Hort 1935;10:17–22.